Comparing AB Model and Emerging Network for Epidemic Spreading

I. Iacopini, L. Lenzi *students at the University of Turin*

In this paper we design and implement an agent-based epidemiological simulation system, using the NetLogo programming language. The epidemic model is an extension of the standard compartmental SIR model (widely studied in literature and analytically solvable). The movement of agents is based on a random walk modified by local forces that represent geographical travel restrictions, and furthermore by the epidemic diffusion itself. We analyze the global emerging system dynamics as a result of the combination of these induced mechanisms. We also generate the aggregated contact network compared with an equivalent random network created using the Erdós Rényi method.

1 Introduction

Nowadays mathematical models represent a compulsory tools for the studying of spreading phenomena in a wild variety of different fields dealing with, for example, rumors and epidemics spreading, opinion dynamics or social interactions in general. In fact epidemics modeling is a very active field of research which crosses different areas, involving computer scientists, epidemiologists and social scientists, investigating the diffusion dynamics of viruses, knowledge, culture, innovation and language. Despite their apparent diversity, all of these problems can be investigated starting from the well known complexity paradigm; complexity in point of fact should be conceived as a condition in which local interactions and agent behavior combine to create new macro outcomes, that could not be predicted from the knowledge of individual behaviors and features of the local interactions alone.

1.1 ABMs and Networks

In social epidemiology two approaches are particularly useful: network analysis and agent-based modeling.

- Networks are a powerful framework for the combined representation of the social structure respect to local and global interactions. Local links cover the description of the human geographical interactions of everyday life and an approximated contact network for every single person. In a similar way, global links cover the description of diffusion processes of population through the global infrastructural network (railways, highways and air transport). For a complete and faithful representation these last links should be developed on different scales: international, intra-nation and intra-city.
- Agent-Based models strongly use stochastic simulation of individuals in a simulated space (often associated with a dual social space). The power of this modeling approach has been to break simplistic assumptions required for mathematical tractability, e.g. homogeneity, ignoring interaction (Axelrod, 1997). One of the most important AB model's feature, often not included but almost mandatory in the field of complex systems,

is the agent's autonomy. This approach allows us to understand how the micro-level behaviors and movements of these independent agents lead to emerging macro-level disease and prevalence distributions.

1.2 Epidemic Models: SIR and SIS

The simplest class of epidemic models is the compartmental model, that assumes that the population can be divided into different classes depending on the stage of the studied disease. The minimal standard framework involves two or three different compartments:

1. Susceptible (denoted by S, those who can contract the infection).

2. Infectious (I , those who have contracted the infection and are contagious).

3. Recovered (R, those who have recovered from the disease).

The dynamics of the individuals between the different compartments depends on the specific characteristics of the disease. The transition from a compartment to the other is triggered by a reaction rate. Usually there are two possible types of elementary processes ruling the disease dynamics. At the beginning there is a little number of seed agents at the state I, while all the other agents begin in the S state. The transition from the S to the I state is governed by the probability β (triggered by the effective proximity of two or more individuals). Every infected agent has a probability μ of spontaneously moving to state R (for the SIR model) or to return to the state S (for the SIS model).
In network analysis the outcomes of these two compartmental epidemic models (e.g. the epidemic threshold and the prevalence curves) are strongly influenced by the specific topology of the considered network.

2 Developing an extended compartmental model

We focus our attention on a more realistic, but still basic, compartmental model (*Figure 1*).
Let introduce four classes:

1. Susceptible (denoted by S, those who can contract the infection).

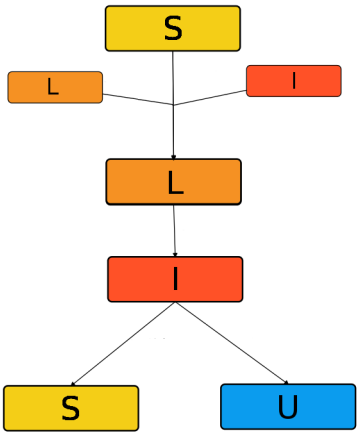

Figure 1: *Diagram of the compartmental model.*

2. Latent (L, those who have contracted the infection and are contagious, but don't exhibit any symptoms).

3. Infectious (I , those who have contracted the infection. They are contagious and do exhibit symptoms).

4. Immune (U, those who have recovered from the disease and are no longer susceptible).

In our model we start with a population of $s = N - u - l$ agents in state S, u agents in state U and a little number l of agents in state L ($l << N$). When a latent agent gets in contact (we will define after what it means) with an S agent he can infect him with probability β. The same thing happens when an agent S gets in contact with an agent I. The transition between the latency phase and the I is spontaneously governed by the decay probability $\frac{1}{\tau}$ (where τ is the mean life time of L state). An infected agent decays with a transition rate μ and furthermore the chance to move into an S state is α_1, while the chance to move into an U state is α_2, such that $\alpha_1 + \alpha_2 = 1$. Finally, the total probability for the transition to an S or U state is $\mu\alpha_1$ and $\mu\alpha_2$, respectively.

The transition rules between different classes are:

$$\boxed{S + L \xrightarrow{\beta} 2L} \tag{1}$$

$$\boxed{L \xrightarrow{\frac{1}{\tau}} I} \tag{2}$$

$$\boxed{S + I \xrightarrow{\beta} L + I} \tag{3}$$

$$\boxed{I \xrightarrow{\mu\alpha_1} S} \tag{4}$$

$$\boxed{I \xrightarrow{\mu\alpha_2} U} \tag{5}$$

In the next section we will implement our model using the NetLogo platform with an AB approach grounded on a random walk subjected to particular restrictions and enforcements, depending on the agent's class and on the geometry of the problem.

2.1 A-B Modeling

We divide the NetLogo grid of patches into M continents, using rigid unassailable barriers containing some crossing gates with variable width. We start the simulation populating the boxes with a number N of agents (instantiated with a random angle), so divided:

- s susceptible agents randomly distributed.
- u immune agents randomly distributed.
- l latent agents randomly distributed in a single box.

At each tick of the simulation the agents obey the following general rules:

Not infected agents randomly sort an angle and a step-length (drawn from an fixed range) and move.

Infected agents act in the same way of the others, but with a lowered mobility caused by their sickness state. The step-length is so drawn from the previous range, properly rescaled.

Contagion: both L and I agents infect each neighboring S agent that stands in his contagion region (a circle of fixed radius) with probability β.

Boundary Condition: when an agent get close to a barrier there's an inelastic scatter that prohibits the crossing of the barrier.

In order to restrict the randomness of the agent's dynamics and stress the model towards a little bit more realistic behavior we also impose the prescriptions explained in the following paragraphs.

2.1.1 Infectious Repulsion

When a not infected agent finds an infected agent in his proximity region (a circle with a fixed radius R *patches* representing the human vision) he turns around of 180 plus a little random extra and moves away with raised mobility.

2.1.2 Flocking Dynamic

The two macro-classes of not infected agents and infected agents obey to the same flocking dynamic [9], but only within its own class. Normally this kind of modeling is referred to swarm dynamics, but in this case it provides an appropriate description of the "general idea" that not infected agents locally bias each other, escaping from the infected ones. The agents follow three rules: alignment, separation, and cohesion.

Alignment means that an agent tends to turn so that it is moving in the same direction that nearby agents are moving. In particular nearby means a circle of a defined radius $r = \frac{R}{2}$ centered on the agent. When an agent finds more than one agents in its circle, it select the nearest and try to align themselves with him; we set the maximum turning angle at 15.

Separation means that an agent will turn to avoid another agent which gets too close (with respect to a minimum-separation threshold $d_{min} = 1$ *patch*).

Cohesion means that an agent will move towards other nearby agents (unless another agent is too close).

When two agents are too close, the separation rule overrides the other two, which are deactivated until the minimum separation d_{min} is achieved. The three rules affect only the agents heading. Each agent always moves forward with the step-length of its own class.

2.1.3 Global Restrictions

In our simulations we set a number $M = 4$ of continents (*Figure 2*). For the sake of simplicity each continent corresponds to a quadrant of the NetLogo grid. We can think of barriers built over the Cartesian axis (from the end of the grid to the center) as geographical restrictions to inter-continent agent's mobility. Given that the agent's movement is essentially a random walk, the gate width is proportional to the net flux of agents between each pair of continents. In this way barriers may represent the travel restrictions imposed by global authorities in presence of an epidemic outcome. In order to get a meaningful behavior we need a functional form for the gate-width w, depending on the number of infected agents i, so that little values of f lead to a

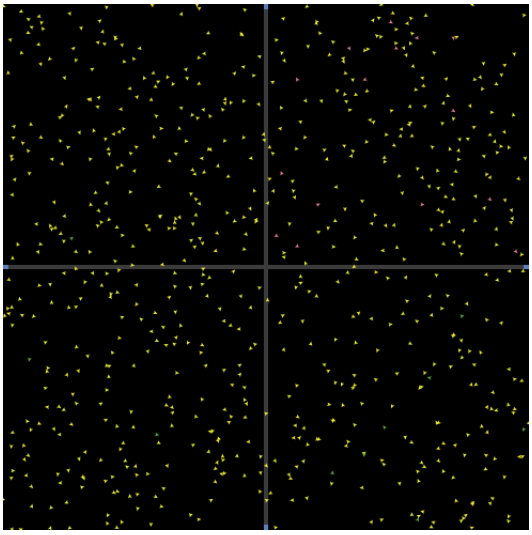

(a) Closed barriers

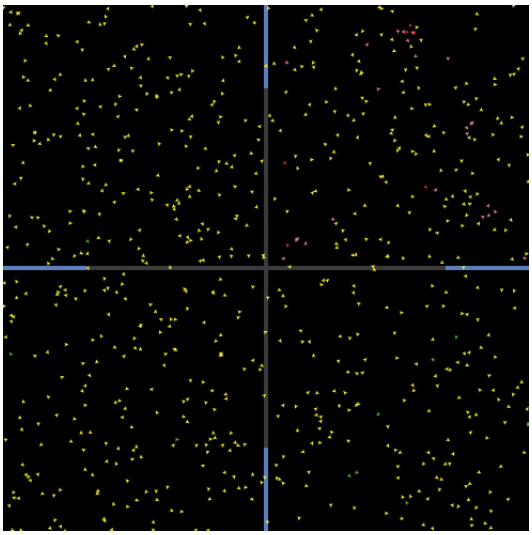

(b) Opening barriers

Figure 2: *Barriers dynamics.*

notable w decrease. A satisfying function for this purpose is the Fermi's Function:

$$w = A\left[1 - \frac{2}{e^{\frac{b}{i}} + 1}\right] \tag{6}$$

where A is a constant tuned on the NetLogo grid.

3 Simulations and Results

During the simulations we focus our attentions mostly on two particular features:

- **Prevalence Curves** They show at each time-step the number of agents that belong to each specific compartment.
- **Lifetime prevalence (LTP)** The fraction of agents that have experienced (at least one time) the infection condition during the simulations.

3.1 Key Parameters

We are interested in the analysis of these two features under variations of the following infection key parameters (previously introduced):

- β, which is the infectivity.
- τ, which controls the mean life of L state.
- μ, which controls the mean life of I state.
- α_1, which controls the probability for a decaying state I to move into a state S.

The remaining parameters of the model are always fixed: $s = 700$, $u = 10$, $l = 15$, $R = 4$.

3.2 Parameters Investigation

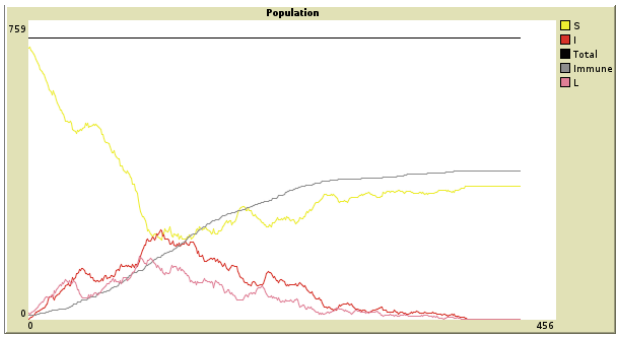

(a) $\alpha_1 = 0.9$

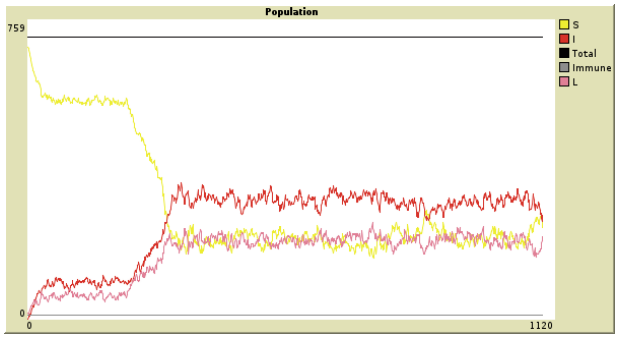

(b) $\alpha_1 = 1$

Figure 3: *Prevalence curves for two different α_1 values. The other key parameters have values: $\beta = 0.68$, $\tau = 7$, $\mu = 0.10$.*

Each key parameter is investigated in turn, while the remaining parameters are fixed at the default values (determined by empirical testing). Despite the fact that this does not catch the correlations between the key parameters, it allows to understand the statistical effect on the prevalence curves.
We focus only in epidemic processes with a transient state, which means that the system always reaches an absorbing state with only S, L or U agents, and

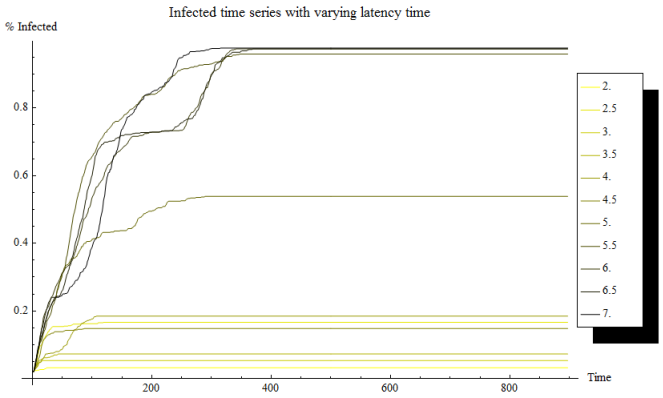

(a) LTP curves as function of time

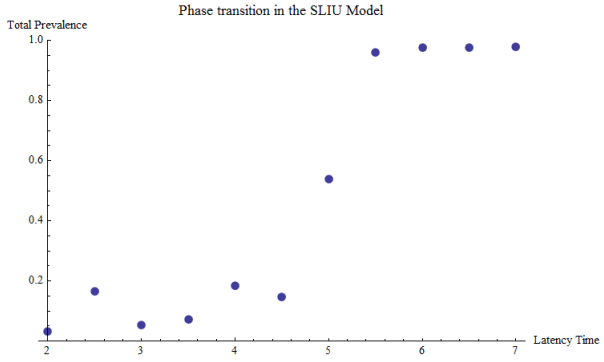

(b) Total LTP as function of τ

Figure 4: *LTP curves as function of time, under variation of parameter τ (a); LTP as function of τ (b). The other key parameters have values: $\beta = 0.68$, $\mu = 0.10$, $\alpha_1 = 0.94$.*

no more infected. This request is always satisfied for $\alpha_1 < 1$ (*Figure 3(a)*). Otherwise the system reaches a stationary state, practically acting as a SIS model (*Figure 3(b)*).

3.3 Results Investigation

Empirical analyzes show the central rule of the τ parameter as dynamic controller (*Figure 4(a)*):

i For a small τ the spreading does not involve the entire "world", but only affects a fraction (not more than two continents). Furthermore, the epidemic rapidly goes towards extinction (*Figure 5(a)*).

ii For a high τ the epidemic wide spreads all over the continents and the mean life of the disease is significantly longer than in the previous case (i) (*Figure 5(b)*).

iii There is an intermediate little range of values for τ where the spreading dynamics is subjected to large stochastic fluctuations, covering the majority of possible outcomes between the two previous regimes (i)(ii).

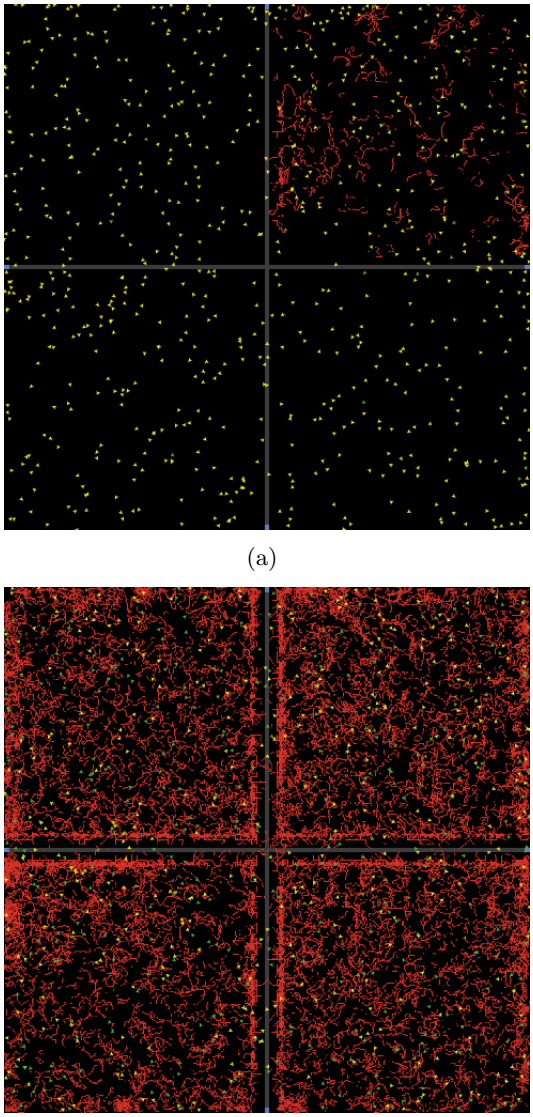

(a)

(b)

Figure 5: *Two different scenarios for different values of parameter τ. The red lines are traces of the passage of I agents.*

This simply happen because the epidemic spreading is mainly driven by the latent agents that still have a complete mobility and are not recognized by the S agents as a danger, but have the same infectivity of the infected ones. Therefore, the L mean life (τ) is crucial: low values prevent L agents from diffuse the disease at large distance, and so the barriers are able to contain the disease in one continent; on the other side, for higher values the action of the barriers can no longer contain the spreading. In the intermediate phase, all scenarios are accessible and the randomness dominates the system dynamics (*Figure*

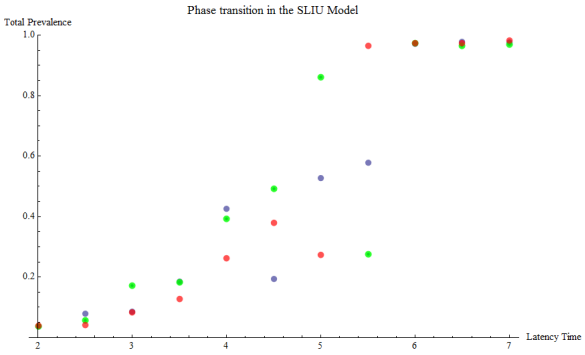

Figure 6: *Overlapping the plot of different simulations for the total LTP as a function of τ. The other key parameters have values: $\beta = 0.68$, $\mu = 0.10$, $\alpha_1 = 0.94$.*

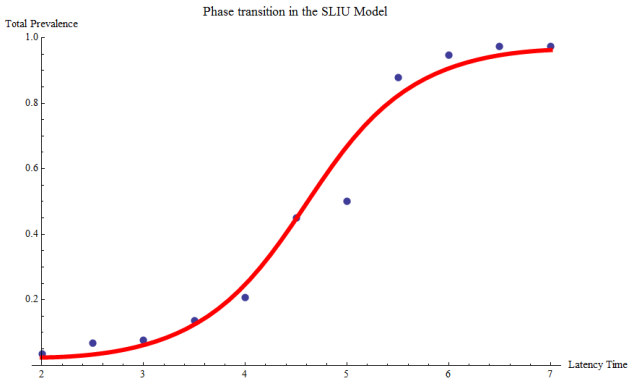

Figure 7: *Mean total LTP as function of τ. The other key parameters have values: $\beta = 0.68$, $\mu = 0.10$, $\alpha_1 = 0.94$.*

6). The analysis of the total LTP (total means that the LTPs are evaluated at the end of simulations) as function of τ (*Figure 4(b)*) permits immediately to visualize the total epidemic diffusion under variation of τ. In this way is easier to recognize the intermediate region, where the stochastic fluctuations are well evident.

In order to better understand the behavior of the model in the intermediate region (iii) we repeat fifty times the same simulation, with fixed parameters, and take the mean value of the total LTP for each τ. The resulting plot is shown in *Figure 7*, where the red line comes from the fitting of the data. The figure clearly confirms that for $\tau \leq 4$ the total LTP remains under the symbolic value of 0.25, which implies that the epidemic spreading is isolated only to a single continent. On the other hand, $\tau \geq 6$ implies a global spreading all over the continents (pointed out by total LTP values, which is always over 0.75). In the intermediate region there is a strictly growing trend that marks the transition between the two completely different scenarios.

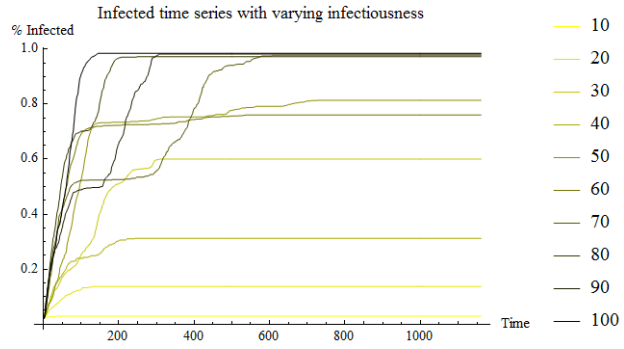

Figure 8: *LTP curves as function of time, under variations of parameter $\beta(\%)$. The other key parameters have values: $\tau = 7$, $\mu = 0.10$, $\alpha_1 = 0.94$.*

Summary of the empirical results:

- $\tau \leq 4$ *leads to regime (i).*
- $\tau \geq 6$ *leads to regime (ii).*
- $4 < \tau < 6$ *leads to regime (iii).*

A decrease in the β value (infectiousness parameter) corresponds to a decrease in the epidemic spreading (*Figure 8*). This is due to the lower capability for the infected and latent agents to vehicular the disease during the contacts with their neighbors. Qualitatively speaking, this implies that as the β decreases, it takes bigger and bigger values of τ in order to make the infection able to reach every continents (i.e. regime (ii)).

The effect of the variation of the μ parameter is simply limited to the temporal duration of the simulation (*Figure 9*). This happens because small μ values only imply an increase in the mean life of the I agents, but, as we previously explained, the spreading dynamics is dominated by the behavior of the L agents, and so the only consequence is a decreasing in the transition rate between I and S/U agents states and finally an increase in the global dynamics time.

Unlike the other parameters, the effects of the α_1 variations are no longer unambiguously interpretable (*Figure 10*). A decreasing in α_1 (remembering that $\alpha_1 + \alpha_2 = 1$) leads to a more rapid growth in the number of immune agents; theoretically this should implies a depletion of the reservoir of susceptible and so a more rapid epidemic extinction. We observe an unexpected rapid and homogeneous diffusion for these low α_1 values and a "zigzagged" growth for higher values. This last effect is due to the well

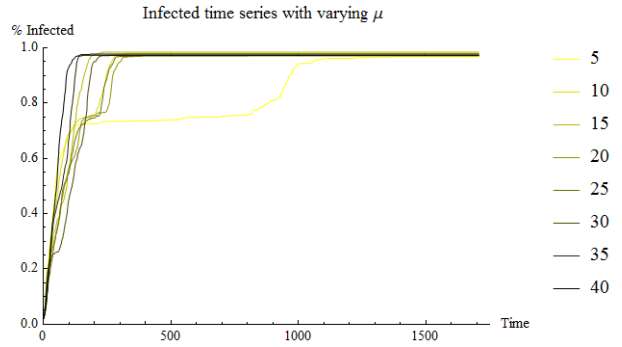

Figure 9: *LTP curves as a function of time, under variations of parameter $\mu(\%)$. The other key parameters have values: $\beta = 0.68$, $\tau = 7$, $\alpha_1 = 0.94$.*

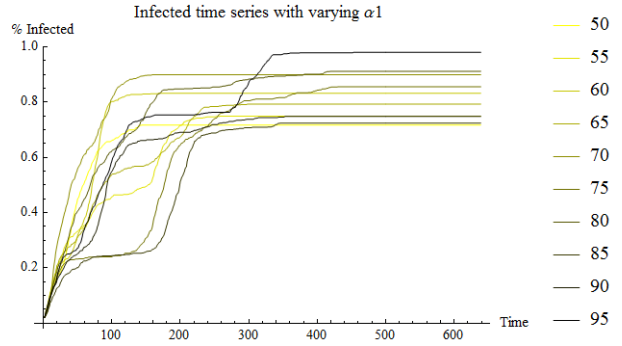

Figure 10: *LTP curves as a function of time, under variations of parameter $\alpha_1(\%)$. The other key parameters have values: $\beta = 0.68$, $\tau = 7$, $\mu = 0.10$.*

known progressive and modular epidemic diffusion through continents. The difference between these two observed behaviors needs further investigations.

4 Emerging Network

In this final section we are going to create the emerging contact network of the agents. Considering that, the basic agent dynamics without disease appearance is practically a random walk, the naturally generated contact network should belong to the random graphs class (i.e. Erdós Rényi). The expected functional form for the degree distribution is a Poissonian:

$$P(k) = \frac{e^{-\mu}\mu^k}{k!} \tag{7}$$

We are interested in understanding how the addition of the epidemic spreading affects this basic dynamic, the network evolution, and the degree distribution at last.

4.1 Network Creation

In order to create the network we consider two different type of contacts:

Proximity contact: when the distance between two agents is less than radius r we define a proximity contact. The first time this happens an undirected edge is created between the involved agents, with weight set up to 1. For every ulterior contact the weight is increased by one.

Repulsive contact: when two agents undergo to a infectious repulsion we define a repulsive contact. For each contact of this type we reduce by two the weight of the shared edge; if the updated values is less than one the link is deleted.

The former contact represents a sort of social relationship between individuals, while the latter represents the weakening of the social interaction due to the appearance of the disease symptoms (a rough sketch of the "survival instinct").
We store all the weights into an adjacency matrix A, where each element a_{ij} represents the edge weight between agents i and j:

$$A = \begin{pmatrix} a_{1,1} & a_{1,2} & \cdots & a_{1,N} \\ a_{2,1} & a_{2,2} & \cdots & a_{2,N} \\ \vdots & \vdots & \ddots & \vdots \\ a_{N,1} & a_{N,2} & \cdots & a_{N,N} \end{pmatrix}$$

A is clearly symmetric and zero-diagonal. The degree of an i-agent k_i is given by:

$$k_i = \sum_{j=1}^{N} a_{ij} = \sum_{i=1}^{N} a_{ji} \tag{8}$$

4.2 Network Analysis

We produce networks over simulations tuned on regime (i) and (ii). From A it is possible to compute the degree distribution. In the first case ($\tau = 3$, (i)) there are some noticeable differences between the obtained degree distribution and the Poissonian one (*Figure 11(b)*). In particular there is a slight densification on the left side of the mean value, while the right-skewed tail represents the presence of an exiguous number of hubs. *Figure 11(a)* shows the final screen-shot of the simulation, with a lower bound over the weights c_w for a better visualization. We can notice a barely appreciable condensation of links on the bottom left corner (continent number 4), belonging to the only continent that has not been infected.

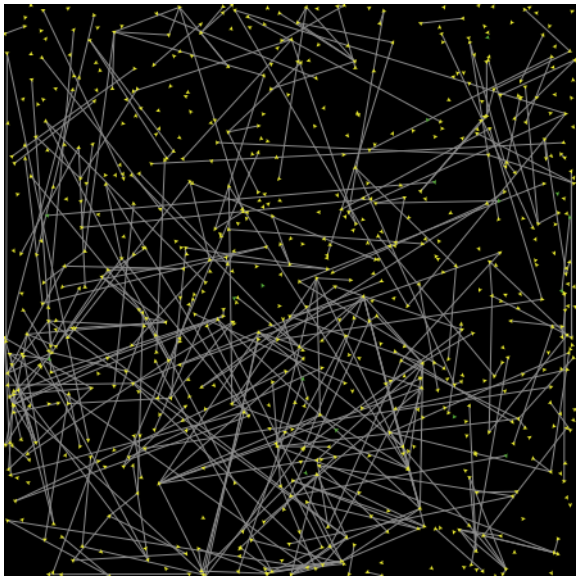

(a) Screenshot

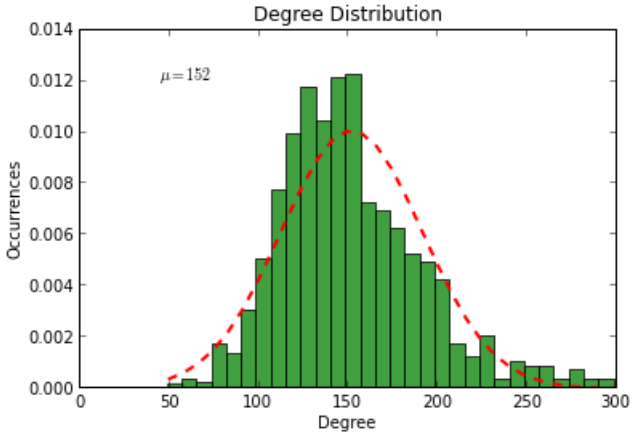

(b) Normed histogram

Figure 11: *Final screen-shot ($c_w = 7$) and histogram of the degree distribution for $\tau = 3$. The other key parameters have values: $\beta = 0.68$, $\mu = 0.10$, $\alpha_1 = 0.94$.*

In the second simulation ($\tau = 7$, (ii)) this last behavior is much more evident. *Figure 12(a)* shows an intermediate screen-shot of epidemic diffusion, where the bottom left corner (4th) has an high density of heavy weighted edges. In fact, we see from the enclosure plot 12(b) that the infection has not reached the fourth continent (the blue curve is at zero level). These heavy weighted edges are also represented by a long right tail observing the associated degree distribution in *Figure 12(c)*.
The final degree distribution in this (ii) regime (*Figure 13(b)*) has the same features already described for the regime (i).

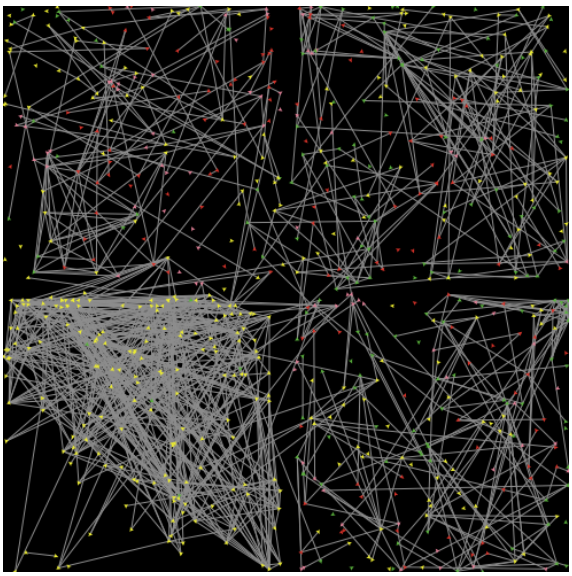

(a) Screenshot

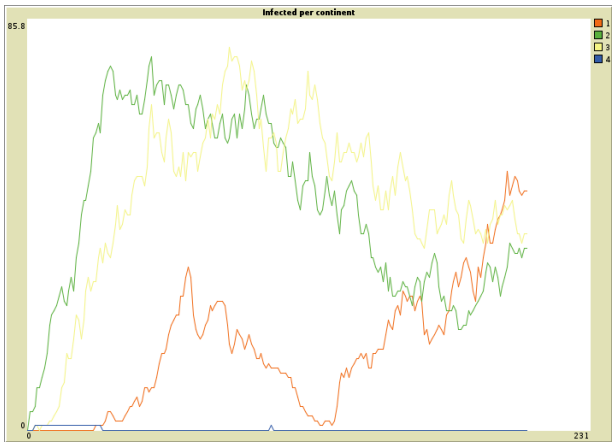

(b) Puntual Prevalence Curves

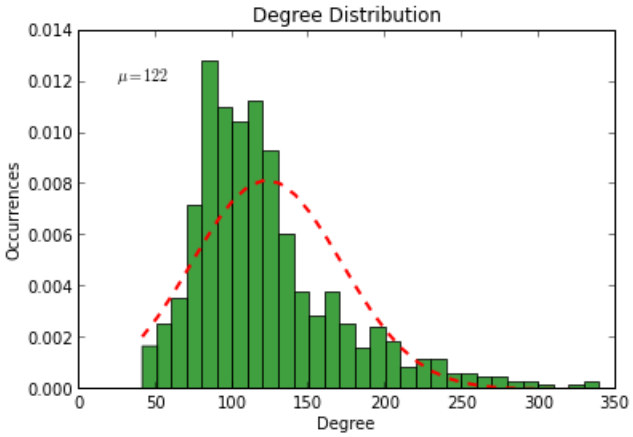

(c) Normed histogram

Figure 12: *Intermediate screen-shot ($c_w = 10$) and related punctual prevalence curves for each continent. The key parameters have values: $\tau = 7$, $\beta = 0.68$, $\mu = 0.10$, $\alpha_1 = 0.94$.*

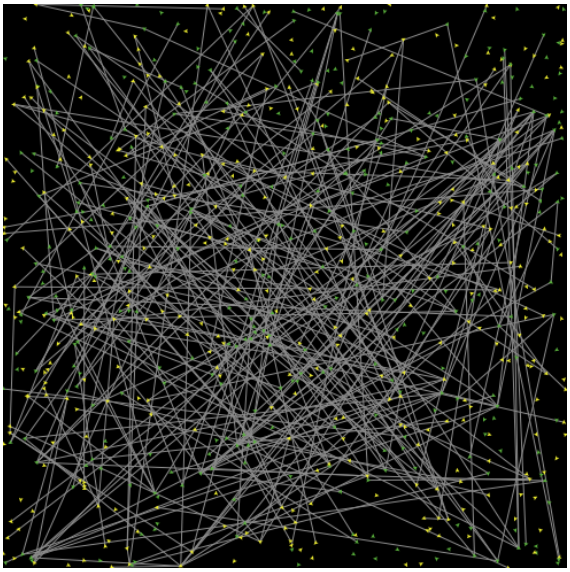

(a) Screenshot

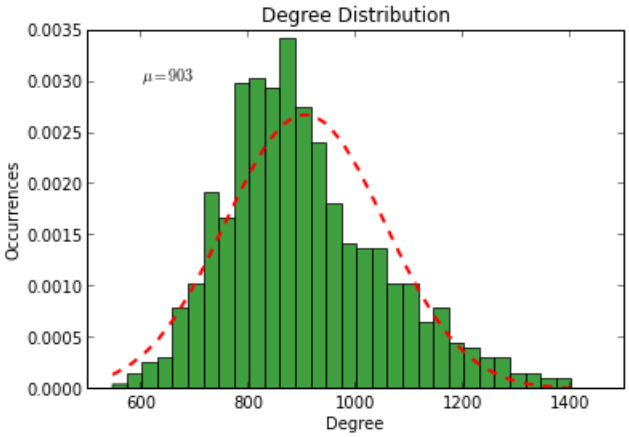

(b) Normed histogram

Figure 13: *Final screen-shot ($c_w = 10$) and histogram of the degree distribution for $\tau = 7$. The other key parameters have values: $\beta = 0.68$, $\mu = 0.10$, $\alpha_1 = 0.94$.*

5 Conclusions

We developed an AB model for epidemic diffusion over a grid. The random work that rules the movement of the agents is altered by the spreading of the disease that introduces new local paired interactions between agents (flocking dynamics, infection repulsion). Furthermore, the inter-continents mobility is modified by the epidemic prevalence itself, according to an exponential law. The alteration of four parameters leads the system to three different global scenarios. Finally, we build the aggregate contact network and from the combined analysis of the degree distribution and the punctual prevalence curve we show the deviation of the emerging network from a standard Erdós Rényi undirected graph. In conclusion, the prevention mechanism involving mobile barriers turns out to be efficient only for a specific set of disease parameters; in the other cases this constraints are not able to confine the spreading. Nevertheless, it is worth remarking that, in a real scenario, the closing of barriers implies a significant interruption of the inter-continent mobility, which represents a severe measure unlikely to be adopted.

References

[1] Shah Jamal Alam and Armando Geller: *Networks in agent-based social simulation.* In *Agent-based models of geographical systems*, pages 199–216. Springer, 2012.

[2] Réka Albert and Albert László Barabási: *Statistical mechanics of complex networks.* Reviews of modern physics, 74(1):47, 2002.

[3] Alain Barrat, Marc Barthelemy, and Alessandro Vespignani: *Dynamical processes on complex networks*, volume 1. 2008.

[4] Vittoria Colizza, Alain Barrat, Marc Barthélemy, and Alessandro Vespignani: *The role of the airline transportation network in the prediction and predictability of global epidemics.* Proceedings of the National Academy of Sciences of the United States of America, 103(7):2015–2020, 2006.

[5] Robert De Caux, Christopher Smith, Dominic Kniveton, Richard Black, and Andrew Philippides: *Dynamic, small-world social network generation through local agent interactions.* Complexity, 2014.

[6] Jill Bigley Dunham: *An agent-based spatially explicit epidemiological model in mason.* Journal of Artificial Societies and Social Simulation, 9(1), 2005.

[7] Magda Fontana and Pietro Terna: *From agent-based models to network analysis (and return): the policy-making perspective.*

[8] Mark EJ Newman: *The structure and function of complex networks.* SIAM review, 45(2):167–256, 2003.

[9] U. Wilensky: *Netlogo flocking model.* Center for Connected Learning and Computer-Based Modeling, Northwestern University, Evanston, IL, 1998.